Peer-reviewed version available at *Int. J. Mol. Sci.* **2020**, *21*, 429; doi:10.3390/ijms21020429

***Title Page (with author names and affiliations)**

Megavoltage radiosensitization of gold nanoparticles on glioblastoma cancer cell line using a clinical platform

Farasat Kazmi[1], Katherine A Vallis[2], Balamurugan A Vellayappan[3], Aishwarya Bandla[4], Duan Yukun[5], Robert Carlisle[6]

Affiliations:

1. Early Phase Clinical Trials Unit, Department of Oncology, University of Oxford, United Kingdom.

2. CRUK/MRC Oxford Institute for Radiation Oncology, University of Oxford, United Kingdom.

3. Department of Radiation Oncology, National University Cancer Institute (NCIS), Singapore.

4. Singapore Institute for Neurotechnology (SINAPSE), National University of Singapore (NUS), Singapore.

5. Department of Chemical and Biomolecular Engineering, National University of Singapore (NUS), Singapore

6. Department of Biomedical Engineering, University of Oxford, United Kingdom.

*** Corresponding Author:**

Dr. Farasat Kazmi, MB BCh BAO LRCP (Ireland), MRCS (UK), MSc in Nanomedicine (Oxford)

Clinical Research Fellow

Early Phase Clinical Trials Unit

Peer-reviewed version available at Int. J. Mol. Sci. 2020, 21, 429; doi:10.3390/ijms21020429

University of Oxford Department of Oncology

Churchill Hospital

Oxford, OX3 7LE. UK

Tel.: +447701087509

Email: farasat.kazmi@oncology.ox.ac.uk

National Cancer Centre Singapore (NCCS),

11 Hospital Dr,

Singapore 169610

Email: Farasat.kazmi@oncology.ox.ac.uk

Conflict of interest statement: The authors declare no conflicts of interest.

Acknowledgements: We thank Dr. Melvin Chua and his team at National Cancer Centre Singapore for providing his laboratory to conduct the clonogenic experiments.

Disclosure: The abstract of this paper was presented at the American Society of Radiation Oncology (ASTRO) 60th Annual Meeting held in San Antonio, October 2018. It was a poster presentation with interim findings. The poster's abstract was published in "Poster Abstracts" in the International Journal of Radiation Oncology. DOI: https://doi.org/10.1016/j.ijrobp.2018.07.675

Word count: 199 (abstract), 3,626 (body text)

ABSTRACT

Gold nanoparticles (GNPs) have demonstrated significant dose enhancement with kilovoltage (kV) X-rays however recent studies have shown inconsistent findings with megavoltage (MV) X-rays. We proposed to evaluate the radiosensitization effect in U87 glioblastoma (GBM) cells in the presence of 42 nm GNPs and irradiated with a clinical 6 MV photon beam. Cytotoxicity and radiosensitization was measured using MTS and clonogenic cellular radiation sensitivity assays respectively. Sensitization enhancement ratio was calculated for 2 Gy (SER_{2Gy}) with GNP (100 μg/mL). Dark field and MTS assay revealed high co-localization and good biocompatibility of the GNPs with GBM cells. Significant sensitization enhancement of 1.45 ($P = 0.001$) was observed with GNP 100 μg/mL. Similarly, at 6 Gy there was significant difference in the survival fraction between GBM alone group (Mean (M) = 0.26, Standard Deviation (SD) = 0.008) and GBM plus GNP group (M = 0.07, SD = 0.05, $P = 0.03$). GNPs enable radiosensitization in U87 GBM cells at 2 Gy when irradiated using a clinical platform. In addition to the potential clinical utility of GNPs, these studies demonstrate the effectiveness of a robust and easy to standardise in-vitro model that can be employed for future studies involving metal nanoparticle plus irradiation.

Keywords: Nanoparticles, Glioblastoma Multiforme, Radiosensitizers, External beam radiotherapy

Peer-reviewed version available at Int. J. Mol. Sci. 2020, 21, 429; doi:10.3390/ijms21020429

1. INTRODUCTION

Glioblastoma (GBM) is one of the most common and aggressive brain cancers in adults, affecting 3 in 100,000 individuals worldwide annually. (1) The current standard of care utilizes a multidisciplinary approach which involves maximal safe tumour resection followed by adjuvant radiotherapy and temozolamide (TMZ), a radiosensitizer.(2) Despite standard treatment, GBM invariably recurs with median progression free survival ranging from 5.5 to 13.0 months.(2) The majority of relapses occur within the high dose radiation treatment field.(3) However, the radiation dose delivered to tumour site is limited by tolerance of the surrounding healthy brain tissue and hence there is an urgent need for novel therapeutics to improve clinical outcomes in these patients.

A major appeal of nanoparticles (NPs) is their ability to deliver cytotoxic agents to the tumour site with increased precision and effectiveness via a phenomenon known as enhanced permeability and retention effect (EPR).(4) Although the true scale of EPR is a topic of contention, it represents a substantial improvement over the delivery of free drug, potentially allowing a higher percentage of the active agent to reach its target, thereby enabling reduced dosing and lower off-target effects.(5) In recent years, gold nanoparticles (GNPs) have also shown great promise to be used as novel radiosensitizers.(6, 7) Extensive preclinical studies have demonstrated significant local enhancement of absorbed dose by the inclusion of GNPs compared to kilovoltage (kV) X-rays alone.(8-10) Indeed, Hainfield was the first to demonstrate radiosensitization effect of 1.9 nm GNPs with 250 kV X-ray using in vivo mouse model. Mice irradiated together with GNPs had 86% 1-year survival contrasting with 20% for X-rays alone.(9) Similarly, Dorsey's group

Peer-reviewed version available at Int. J. Mol. Sci. 2020, 21, 429; doi:10.3390/ijms21020429

also demonstrated dose enhancement of 30% with 13 nm GNPs incubated in U251 GBM cells when targeted with 150 kV X-ray.(11) These findings have been further validated with existing in vitro and in vivo experiments using different cancer cell lines.(12, 13) The phenomenon driving the impact of GNP is known as the photoelectric effect and has been attributed to the high atomic number of gold (Z = 79) resulting in high mass energy coefficient relative to soft tissue.(9) More specific to U87 GBM cells, Chen recently reported a dose enhancement of 1.37 with bovine serum albumin capped 28 nm GNPs incubated in U87 GBM when irradiated 160 kV X-ray.(14) Using in vivo mouse model, he demonstrated tumour regression by approximately 35% compared RT alone.(14)

However, in a clinical setting, kilovoltage X-rays have limited utility in radiotherapy as they have low dose depth penetration and are unable to deposit radiation dose to deep-seated tumour sites.(6) To overcome this, megavoltage (MV) X-rays, in the range of 4 to 10 MV are used as they provide deeper dose penetration.(7) Predictive models, such as Monte Carlo simulation, have shown that no significant radiosensitization effects occur, with GNPs, in the MV range.(6, 7) However, recent in-vitro experiments have demonstrated varying dose enhancement with GNPs (between 1.16 and 1.5), questioning the validity of these predictive models.(15-17) To account for these differences, it has been proposed that there may be an underlying biological effect exerted by GNPs which has not been well characterized.(10)

To date, there is little standardisation of the RT techniques and models which have been used to produce MV X-rays to conduct these experiments, hence

Preprints (www.preprints.org) | NOT PEER-REVIEWED | Posted: 28 October 2019 doi:10.20944/preprints201910.0318.v1

Peer-reviewed version available at Int. J. Mol. Sci. 2020, 21, 429; doi:10.3390/ijms21020429

comparison between studies is challenging.(18) A lack of clarity is a consequence of all these factors, and the clinical translation of GNPs as radiosensitizers has faced significant setbacks. The primary aim of this study is to investigate the radiosensitization effects of GNPs on U87 human glioblastoma (GBM) cells using a 6 MV X-ray generated via use of an easy to establish and standardise clinical linear accelerator (LINAC).

2. MATERIALS AND METHODS

2.1 Cell lines and culture

U87 human Glioblastoma (GBM) cell line was obtained from American Type Culture Collection (ATCC) cultured using 20 mL of Dulbecco's modified Eagle's medium (DMEM), supplemented by 10% fetal bovine serum, 1% antibiotic mixture containing penicillin (Sigma-Aldrich), and streptomycin (Sigma-Aldrich). The cells were plated in T75 flask (Thermo Fisher) and allowed to form a primary monolayer and stored at humidified atmosphere at 37°C with 5% CO_2. The medium was changed every two days. Once the cells reached 80% confluency, the medium was removed and the cell were washed three times with 10 mL of PBS. Subsequently, the cells were detached from the flask using 4 mL of Trypsin-EDTA and stored at 37°C incubator with humidified atmosphere of 5% CO_2 for 5 mins. Next, the cells are suspended in 6 mL of DMEM and split (1:10), transferring 1 mL of the suspension to a new T75 flask with 20 mL of DMEM.

2.2 Gold nanoparticle synthesis and characterization

Gold nanoparticles (GNPs) were fabricated following the classical method introduced by Turkevich.(19) 100 mL 0.01% chlorauric acid (HAuCl4:4H2O)

Peer-reviewed version available at Int. J. Mol. Sci. 2020, 21, 429; doi:10.3390/ijms21020429

solution was refluxed and 1 mL 1% sodium citrate solution was added respectively to the boiling solution. The reduction of gold ions by the citrate ions was completed after 5 minutes. The solution was further boiled for 30 minutes, and then left to cool at room temperature. Impurities were removed using dialysis with membrane of 12-14 kD molecular weight cut-off (MWCO) for 72 hours against ultrapure water. This step ensured removal of all the ions and other unreacted reactants in the colloidal solution.

The hydrodynamic diameter (HD) distributions and Zeta potential of gold nanoparticles were determined by dynamic light scattering (DLS) using a NanoZS Zetasizer (Malvern). The DLS data were acquired in the phase analysis light scattering mode at 25°C, and the sample solutions were prepared by dissolving the GNPs in 10 mM phosphate-buffered saline (PBS) solution (pH 7.0). The size and morphology of GNPs were analysed by transmission electron microscopy (TEM) using a Hitachi HF-2000 field emission high-resolution TEM operating at 200 kV. The Stability of GNPs was evaluated using optical UV-vis absorption spectra. It was recorded on a UV-1800 spectrophotometer (Shimadzu). The photoluminescence (PL) spectra were measured by a F4600 fluorescence spectrophotometer (Hitachi).

2.3 MTS assay

To assess for GNP toxicity on GBM alone, cell viability was measured at 3 h and 24 h post GNP exposure using CellTiter 96 Aqueous One Solution Cell Proliferation Assay kit MTS assay (Promega). 5×10^3 cells (100 µL per well) were seeded in triplicates with 200 µL of DMEM in the 96-well plates and stored in the

Peer-reviewed version available at *Int. J. Mol. Sci.* **2020**, *21*, 429; doi:10.3390/ijms21020429

incubator overnight at humidified atmosphere at 37°C with 5% CO_2. Next, the cells were washed with PBS and the medium was replaced with fresh medium containing different concentration of GNPs (50 µg/mL, 100 µg/mL) and medium only (GBM cell with no GNP). After 3 h, medium was removed and cells were washed with PBS twice. Next, 20 µl MTS was added to each well and incubated for 1 h. The optical density (OD) was recorded at 490 nm in a 96-well plate reader (Biorad). The experiment was repeated to assess for cytoxicity at 24 h. Cell viability was expressed as percentage of the absorbance value of the GNP treated group to GBM alone group. Data was a representation of 3 independent experiments (n =3) for each group (3 h and 24 h post GNP exposure).

2.4 Dark field microscopy

In accordance with the work of Manjari's group, who demonstrated the uptake of GNPs into U87 GBM, the following procedure was followed to load cells with GNPs.(20) At 80% confluence, a total of 1 x 10^4 cells were seeded on 6 well plate coverslips for 24 hours. Next, they were dosed with different concentrations of GNP (50 µg/mL and 100 µg/mL) and left overnight at 37°C with 5% CO_2. The following day, cells were washed two times with PBS to remove excess GNPs and fixed with 4% formaldehyde for 5 minutes and washed again three times with PBS. Mounting solution (oregano limonene) was added and left over overnight to dry. The absence of excess GNPs in media or on plastic-ware validated the effectiveness of the washing and the punctate distribution of the GNPs within the cells indicated cell uptake rather than residence of the particles on the surface. Dark field images were taken using an Olympus BX-53 with a dry condenser (U-DCD) and an oil

Preprints (www.preprints.org) | NOT PEER-REVIEWED | Posted: 28 October 2019 doi:10.20944/preprints201910.0318.v1

Peer-reviewed version available at *Int. J. Mol. Sci.* **2020**, *21*, 429; doi:10.3390/ijms21020429

immersion condenser (U-DCW) with objective lens 10x and 100x lens (NA1.2-1.4) respectively.

2.5 Irradiation setup

Radiation doses were delivered as single fraction (2, 4, 6 and 8 Gy) using 6 MV X-rays with TrueBeam® Linac (Varian, Radiotherapy System), at a dose rate of 600 MU/min. A source-axis-distance (SAD) = 100 cm and 10 × 15 cm^2 field size. A Bolus of 5 cm thickness was placed on the top of the plate to serve as a build-up material for the 6 MV beam. A plastic phantom 30 × 30 cm^2 with 8 cm thickness was placed below for back scatter dose. The setup was put through a computed tomography (CT) simulation. Radiotherapy planning (Eclipse™ Treatment Planning System) was done using a 3-field planning technique (2 lateral opposed fields and single anterior field) to provide a homogenous dose distribution. Well plates were encompassed by the 95% isodose line. The setup is shown in figure 1.

2.6 Clonogenic assay

Clonogenic assay was performed to compare 2 groups: GBM cells treated with GNPs (100 µg/mL) versus GBM cells alone. Experiments were carried on a 6-well plate. At 80% confluence, 3 x 10^4 cells were seeded per well for 24 hours. Next, they were incubated with the GNPs (100 µg/mL) overnight. Subsequently, they were irradiated the following day. Radiation was delivered using single doses: 2, 4, 6 and 8 Gy using a LINAC. Immediately after irradiation, 2,000 cells were seeded in each well plate and incubated at 37°C with 5% CO_2 for 10 days or until colonies of greater than 50 cells had been formed. After sufficient colonies had formed, DMEM was removed, washing performed three times with 1 mL PBS, and 500 µL

Preprints (www.preprints.org) | NOT PEER-REVIEWED | Posted: 28 October 2019 doi:10.20944/preprints201910.0318.v1

Peer-reviewed version available at Int. J. Mol. Sci. 2020, 21, 429; doi:10.3390/ijms21020429

of 10% (v/v) neutral-buffered formalin with 50 µL of crystal violet added to each well for 60 minutes at room temperature. Next, the formalin–crystal violet mixture was removed with repeated washing using deionized water. Colonies of 50 cells or more were counted manually and surviving fractions were calculated dividing the plating efficiency of GNP (100 µg/mL) treated cells by plating efficiency of GBM alone (No GNP). Experiment was repeated for an additional two times to have a total of three independent experiments (n = 3). Survival fraction (SF) was calculated based on the following equations: (21)

$$(1)\ \mathrm{PE} = \frac{\text{Number of colonies counted}}{\text{Number of cells}}\ \mathrm{X}\ 100$$

Where PE is the plate efficiency. All the PEs of the treated samples are normalized to that of the control non-irradiated plates.

$$(2)\ \mathrm{SF} = \frac{\text{PE of treated sample}}{\text{PE of control}}\ \mathrm{X}\ 100$$

Survival fraction (SF) results were fit with a linear-quadratic (LQ) model, represented by equation (2). Data was generated using GraphPad Prism 8.0 and plotted on a log (% survival) vs dose plot.

$$(3)\ \mathrm{S} = \mathrm{e}^{-\alpha\mathrm{D} - \beta\mathrm{D}^2}$$

Where S is the survival fraction, α and β are the model constants, and D is the absorbed dose in Gy.

Peer-reviewed version available at Int. J. Mol. Sci. 2020, 21, 429; doi:10.3390/ijms21020429

2.7 Sensitization enhancement ratio

The sensitization enhancement ratio (SER_{2GY}) was determined as the ratio of survival fractions without and with GNPs (100 µg/mL) at 2 Gy. This was based on previous data that have shown that the initial slope of the survival curve, rather than the final slope correlates well with clinical outcomes.(22, 23). 2 Gy also represents the typical individual dose of conventional radiotherapy fractionation delivery.(24)

2.8 Statistical analysis

Differences between GNP-treated and control groups were calculated using an independent sample t-test and one-way analysis of variance (ANOVA) with post-hoc Tukey test using SPSS, with P value of less than 0.05 set to be considered significant. The correlation r^2 values were calculated from the Pearson correlation coefficient using Prism 8.0 (GraphPad Software, CA). For clonogenic assay, data was a representation of 3 independent experiments (n = 3). All results were expressed as mean ± Standard Deviation (SD).

3. RESULTS

3.1 Fabrication and characterization of gold nanoparticles

Figures 2A and 2B show TEM images of GNPs. In terms of size distribution, the polydispersity index (PDI) was 0.302 with size, approximately 41.5 ± 1.98 nm as shown by figure 2C. A zeta potential of -42.03 mV further confirmed that GNPs in this sample were electrically stable ensuring good colloidal dispersion. UV-vis spectroscopy showed that GNPs exhibited strong absorption peaks at 531 nm resulting from their characteristic surface plasmon resonance as shown by figure 2D.

3.2 Gold nanoparticles association with U87 GBM cells

Exposure and biocompatibility of GBM cells to GNPs has previously been reported.(20) The goal of dark field microscopy in this study was to confirm interaction of GNPs by the U87 GBM cells. Figure 3A confirms this with observation of GNPs association with cells evident at all tested concentrations (25 µg/mL, 50 µg/mL and 100 µg/mL). Higher concentrations correlated with increased association, with 100 µg/mL GNPs having a substantially increased density of GNP clustering within GBM cells. From these results, we are unable to definitively ascertain GNP uptake in cytosol compared to nucleus. Notably, nuclear association may be required for optimal impact of Auger emission. (25)

3.3 Cytotoxicity of gold nanoparticles in the absence of radiation

Before the impact of radiation on cells with GNPs could be ascertained, it was important to establish the 'background' level of toxicity associated with exposure of cells to the GNPs alone as shown by figure 3B. U87 GBM cells were incubated with increasing concentration of GNPs and cell viability was assessed with MTS assays at 3 h and 24 h respectively. Cell viability remained greater than 90% in all GNP treated groups, 50 µg/mL and 100 µg/mL GNP, with no statistically different viability levels evident in any group (at 3 h $P = 0.28$, 24 h $P = 0.261$) and no dose toxicity relationship evident.

3.4 Clonogenic assay and sensitization enhancement ratio

Peer-reviewed version available at Int. J. Mol. Sci. 2020, 21, 429; doi:10.3390/ijms21020429

The most robust means of quantifying radiation induced cell death is to study the ability of cells to form and grow colonies post exposure (see methods). U87 GBM cells incubated with GNPs (100 µg/mL) demonstrated a radiosensitization effect, compared to those exposed to RT alone, as shown by figure 4A and the images in figure 4B. Notably, the survival fraction (SF) at 2 Gy was significantly higher for GBM alone group (Mean (M) = 0.88, SD = 0.05) versus the GNP (100 µg/mL) treated group (M = 0.61, SD = 0.06, P = 0.004). The sensitization enhancement ratio with GNP at 2 Gy (SER_{2Gy}) was therefore 1.45. At 6 Gy, substantial and significant enhanced cell kill was seen with the GNP group giving a SF value 4-fold lower (M = 0.07, SD = 0.05, P = 0.03) compared to GBM alone (M= 0.26, SD = 0.008). Interestingly, this level of kill was not matched even by exposure to 8 Gy in GBM alone group. At 4 Gy, the trend of decreased SF was also seen in the GNP group compared to GBM, but the effect did not reach significance (GNP group M = 0.35, SD = 0.11 vs GBM alone group M = 0.49, SD = 0.21, P = 0.33), due to the large variation at this dose. Finally, at 8 Gy dose response was noted again showing similar trend with increased cell kill in GNP group (M = 0.083, SD = 0.068, P = 0.322) compared to GBM alone (M = 0.131, SD = 0.027) but not to a statistically significant level.

4. DISCUSSION

In this study, we have demonstrated a significant radiosensitization effect with SER_{2Gy} 1.45 (P = 0.004) with 42 nm GNPs at high concentrations (100µg/mL) in U87 GBM cell line with megavoltage radiation. A simple and fast one-step synthesis method was used to fabricate the GNPs without need for complex surface modifications to achieve the radiosensitization effect. Dark field microscopy

Peer-reviewed version available at Int. J. Mol. Sci. 2020, 21, 429; doi:10.3390/ijms21020429

revealed high co-localization and biocompatibility of the GNPs within the GBM cells. The rationale behind utilizing 42 nm GNP in this experiment was based on a study by Chitrani's group that demonstrated 50 nm GNPs exhibited the highest radiosensitization in HeLa cells compared to 14 nm and 74 nm GNPs when irradiated with 220 kVp X-rays, DEF of 1.43 compared to 1.2 and 1.25, respectively.(26) In addition, various reports have shown relative safety of GNPs in the range of 20 nm – 50 nm in different cell lines. (27, 28). A recent in vitro study demonstrated no GNP associated toxicity on HepG2 cells when incubated with 20 and 50 nm GNPs.(29) However, in the same study, 5 nm GNP exerted significant genotoxicity in a dose dependant manner.(29)

From our literature review, we did not find any in-vitro study investigating the MV radiosensitization in U87 glioblastoma cell lines. We feel that this is an important area of investigation in view of the radio-resistance that is commonly seen in GBM, compared to other cancer types, and the fact that MV radiation is more clinically appropriate than kV. Several groups have reported significant MV radiosensitization in various other cancer cell lines. Jain and co-workers were one of the first groups to demonstrate significant radiosensitization in MDA-MB-231 cells, SER_{2Gy} 1.29 and 1.16 with 6 MV and 15 MV X-rays respectively.(15) In-vitro studies by Chithrani also demonstrated similar outcomes, i.e. radiosensitivity enhancement factor (REF) 1.17, with 50 nm GNPs incubated in HeLa cells using 6 MV X-rays.(26) Similarly, Liu et al demonstrated significant radiosensitization with 6.1 nm PEGylated GNP incubated in CT26 cells and irradiated with 6 MV X-ray.(30) Based on the survival curves in the paper, we deduced the estimated SER_{2Gy} (ratio of survival fractions without and with GNPs) was 1.40 for 500 µM

Preprints (www.preprints.org) | NOT PEER-REVIEWED | Posted: 28 October 2019 doi:10.20944/preprints201910.0318.v1

Peer-reviewed version available at Int. J. Mol. Sci. 2020, 21, 429; doi:10.3390/ijms21020429

PEGylated GNP which was similar to the SER_{2Gy} value of 1.45 that we observed in this study.(30) Interestingly, Liu also demonstrated a direct correlation with radiosensitization effect and increasing GNP colloidal concentration.(30, 31)

These results are aligned with our findings that indeed MV radiation does exert significant dose enhancement at the target site. However, we also noted contrasting reports regarding the MV radiosensitization with GNPs. Sara et al reported results of a direct comparison of radiosensitization achieved between 160 kV versus 6 MV X-rays on platinum-sensitized F98 glioma cells.(32) She demonstrated DEF 1.81 following irradiation with 160-kV X-rays compared with 1.14 for 6 MV photons.(32) In this scenario, we would expect for higher radiosensitization with MV X-rays especially when delivered concurrently with a platinum radiosensitizer. Several reasons could explain these findings. Firstly, from our experience, radiotherapy dosimetry for MV planning using a single anterior or posterior field generally results in significant dose heterogeneity hence these results may not be reflective a homogenously irradiated sample.(32) Secondly, RT was delivered using a single dose of 7 Gy which may indeed be a maximum tumourcidal dose and GNP may not add any meaningful enhancement at such a high dose.(32) We also noted similar findings with our colony forming assay at the 8 Gy dose point as shown by figure 4.

Despite, these findings, it is important to note that there is a lack of a unified metric to characterize radiation effects in the literature. This has led to vast diversity in defining radiosensitization. Studies have used dose enhancement factor (DEF), radiosensitivity enhancement factor (REF), dose modifying factor (DMF) interchangeably to describe radiosensitization effects as a ratio of doses to achieve

Peer-reviewed version available at *Int. J. Mol. Sci.* **2020**, *21*, 429; doi:10.3390/ijms21020429

the same effect hence making it difficult for direct comparison. (6, 11, 15, 33) Our rationale for using SER_{2G} was to reflect the clinical setting, as the standard radiotherapy regimen for glioblastoma is to deliver 60 Gy in 30 fractions (2 Gy per fraction) to the target volume.(2)

The strength of this study are as follows: we used a simple yet robust model to study radiosensitization on bare GNPs using a clinical LINAC. We strongly advocate the use of a simple 3-field RT delivery technique as it overcomes any dose inhomogeneity that would otherwise result from air gaps between the lid and the medium as shown by figure 1 and so would help standardise experiments performed at different centres using a LINAC to irradiate samples. Secondly, we used the 'gold standard' clonogenic assay method to determine primary cell survival curves with good accuracy using 4 RT dose points (2 – 8 Gy). The clonogenics also validated our 3-field model as we observed a tumour dose response as shown by 4b.

A number of limitations need to be mentioned. Firstly, although demonstration of co-localization of GNPs with the GBM cells was achieved, it is difficult to assess the true yield of intracellular uptake based on dark field experiments and there is no confirmation that the GNPs are located in perinuclear space where they could generate the greatest impact.(6) Hence, this issue may be addressed in future studies to optimise the effect achieved, potentially by surface modification of the gold. Secondly, there was a lack of comparison to GNP group with different concentrations so it would be difficult to establish radiosensitization correlation to GNP concentration. Finally, functional assays, such as H2AX, are needed as it would provide more insights to the mechanism cell kill. However, due to the

Preprints (www.preprints.org) | NOT PEER-REVIEWED | Posted: 28 October 2019 doi:10.20944/preprints201910.0318.v1

Peer-reviewed version available at Int. J. Mol. Sci. 2020, 21, 429; doi:10.3390/ijms21020429

complex nature of metal oxide nanoparticles and their interactions with photons, we wanted to first establish a robust model prior to delving more into understanding the mechanism of action.

In conclusion, we have demonstrated a significant GNP radiosensitization in U87 GBM cell lines using a clinical platform. In addition, we demonstrated the advantage of using a 3 field RT technique that has not been described prior to this study using in-vitro model. Although, these results are promising, further understanding of the mechanism of radiosensitization is needed. For example, it would be interesting to quantify ROS generation and DNA double strand breaks using a robust experimental model, similar to this experiment. Finally, additional in vivo experiments will hopefully help define the ultimate clinical utility of delivering GNPs to tumour sites.

REFERENCES

1. Thakkar JP, Dolecek TA, Horbinski C, Ostrom QT, Lightner DD, Barnholtz-Sloan JS, et al. Epidemiologic and molecular prognostic review of glioblastoma. Cancer Epidemiol Biomarkers Prev. 2014;23(10):1985-96.
2. Stupp R, Mason WP, Van Den Bent MJ, Weller M, Fisher B, Taphoorn MJ, et al. Radiotherapy plus concomitant and adjuvant temozolomide for glioblastoma. New England Journal of Medicine. 2005;352(10):987-96.
3. Catterall M, Bloom H, Ash D, Walsh L, Richardson A, Uttley D, et al. Fast neutrons compared with megavoltage x-rays in the treatment of patients with supratentorial glioblastoma: a controlled pilot study. Int J Radiat Oncol, Biol Phys;(United States). 1980;6(3).
4. Maeda H, Wu J, Sawa T, Matsumura Y, Hori K. Tumor vascular permeability and the EPR effect in macromolecular therapeutics: a review. Journal of controlled release. 2000;65(1-2):271-84.
5. Wilhelm S, Tavares AJ, Dai Q, Ohta S, Audet J, Dvorak HF, et al. Analysis of nanoparticle delivery to tumours. Nature reviews materials. 2016;1(5):16014.
6. Butterworth KT, McMahon SJ, Taggart LE, Prise KM. Radiosensitization by gold nanoparticles: effective at megavoltage energies and potential role of oxidative stress. Translational Cancer Research. 2013;2(4):269-79.
7. Cui L, Her S, Borst GR, Bristow RG, Jaffray DA, Allen C. Radiosensitization by gold nanoparticles: will they ever make it to the clinic? Radiotherapy and Oncology. 2017;124(3):344-56.
8. Zhang X-D, Wu D, Shen X, Chen J, Sun Y-M, Liu P-X, et al. Size-dependent radiosensitization of PEG-coated gold nanoparticles for cancer radiation therapy. Biomaterials. 2012;33(27):6408-19.
9. Hainfeld JF, Dilmanian FA, Zhong Z, Slatkin DN, Kalef-Ezra JA, Smilowitz HM. Gold nanoparticles enhance the radiation therapy of a murine squamous cell carcinoma. Physics in Medicine & Biology. 2010;55(11):3045.
10. Ghita M, McMahon SJ, Taggart LE, Butterworth KT, Schettino G, Prise KM. A mechanistic study of gold nanoparticle radiosensitisation using targeted microbeam irradiation. Scientific reports. 2017;7:44752.
11. Joh DY, Sun L, Stangl M, Al Zaki A, Murty S, Santoiemma PP, et al. Selective targeting of brain tumors with gold nanoparticle-induced radiosensitization. PloS one. 2013;8(4):e62425.
12. Chattopadhyay N, Cai Z, Kwon YL, Lechtman E, Pignol JP, Reilly RM. Molecularly targeted gold nanoparticles enhance the radiation response of breast cancer cells and tumor xenografts to X-radiation. Breast cancer research and treatment. 2013;137(1):81-91.
13. Liu CJ, Wang CH, Chen ST, Chen HH, Leng WH, Chien CC, et al. Enhancement of cell radiation sensitivity by pegylated gold nanoparticles. Physics in medicine and biology. 2010;55(4):931-45.
14. tu y, Chen N, Yang W, Bao Y, Xu H, Qin S. BSA Capped Au Nanoparticle as An Efficient Sensitizer for Glioblastoma Tumor Radiation Therapy. RSC Adv. 2015;5.
15. Jain S, Coulter JA, Hounsell AR, Butterworth KT, McMahon SJ, Hyland WB, et al. Cell-specific radiosensitization by gold nanoparticles at megavoltage radiation

Peer-reviewed version available at Int. J. Mol. Sci. 2020, 21, 429; doi:10.3390/ijms21020429

energies. International Journal of Radiation Oncology* Biology* Physics. 2011;79(2):531-9.
16. Maggiorella L, Barouch G, Devaux C, Pottier A, Deutsch E, Bourhis J, et al. Nanoscale radiotherapy with hafnium oxide nanoparticles. Future oncology. 2012;8(9):1167-81.
17. Cho SH. Estimation of tumour dose enhancement due to gold nanoparticles during typical radiation treatments: a preliminary Monte Carlo study. Physics in Medicine & Biology. 2005;50(15):N163.
18. Hau H, Khanal D, Rogers L, Suchowerska N, Kumar R, Sridhar S, et al. Dose enhancement and cytotoxicity of gold nanoparticles in colon cancer cells when irradiated with kilo‐and mega‐voltage radiation. Bioengineering & translational medicine. 2016;1(1):94-102.
19. Kimling J, Maier M, Okenve B, Kotaidis V, Ballot H, Plech A. Turkevich method for gold nanoparticle synthesis revisited. The Journal of Physical Chemistry B. 2006;110(32):15700-7.
20. Bhamidipati M, Fabris L. Multiparametric assessment of gold nanoparticle cytotoxicity in cancerous and healthy cells: the role of size, shape, and surface chemistry. Bioconjugate chemistry. 2017;28(2):449-60.
21. Franken NA, Rodermond HM, Stap J, Haveman J, Van Bree C. Clonogenic assay of cells in vitro. Nature protocols. 2006;1(5):2315.
22. Kaur H, Pujari G, Semwal MK, Sarma A, Avasthi DK. In vitro studies on radiosensitization effect of glucose capped gold nanoparticles in photon and ion irradiation of HeLa cells. Nuclear Instruments and Methods in Physics Research Section B: Beam Interactions with Materials and Atoms. 2013;301:7-11.
23. Deacon J, Peckham M, Steel G. The radioresponsiveness of human tumours and the initial slope ofthe cell survival curve. Radiotherapy and Oncology. 1984;2(4):317-23.
24. Subiel A, Ashmore R, Schettino G. Standards and methodologies for characterizing radiobiological impact of high-Z nanoparticles. Theranostics. 2016;6(10):1651.
25. McQuaid HN, Muir MF, Taggart LE, McMahon SJ, Coulter JA, Hyland WB, et al. Imaging and radiation effects of gold nanoparticles in tumour cells. Scientific Reports. 2016;6:19442.
26. Chithrani DB, Jelveh S, Jalali F, van Prooijen M, Allen C, Bristow RG, et al. Gold nanoparticles as radiation sensitizers in cancer therapy. Radiation research. 2010;173(6):719-28.
27. May S, Hirsch C, Rippl A, Bohmer N, Kaiser JP, Diener L, et al. Transient DNA damage following exposure to gold nanoparticles. Nanoscale. 2018;10(33):15723-35.
28. Tsoli M, Kuhn H, Brandau W, Esche H, Schmid G. Cellular uptake and toxicity of Au55 clusters. Small (Weinheim an der Bergstrasse, Germany). 2005;1(8-9):841-4.
29. Xia Q, Li H, Liu Y, Zhang S, Feng Q, Xiao K. The effect of particle size on the genotoxicity of gold nanoparticles. Journal of Biomedical Materials Research Part A. 2017;105(3):710-9.
30. Liu C-J, Wang C-H, Chen S-T, Chen H-H, Leng W-H, Chien C-C, et al. Enhancement of cell radiation sensitivity by pegylated gold nanoparticles. Physics in Medicine & Biology. 2010;55(4):931.
31. Liu CJ, Wang CH, Chien CC, Yang TY, Chen ST, Leng WH, et al. Enhanced x-ray irradiation-induced cancer cell damage by gold nanoparticles treated by a new synthesis method of polyethylene glycol modification. Nanotechnology. 2008;19(29):295104.

32. Lim SN, Pradhan AK, Barth RF, Nahar SN, Nakkula RJ, Yang W, et al. Tumoricidal activity of low-energy 160-KV versus 6-MV X-rays against platinum-sensitized F98 glioma cells. Journal of radiation research. 2015;56(1):77-89.
33. Taggart LE, McMahon SJ, Currell FJ, Prise KM, Butterworth KT. The role of mitochondrial function in gold nanoparticle mediated radiosensitisation. Cancer nanotechnology. 2014;5(1):5.

Peer-reviewed version available at *Int. J. Mol. Sci.* **2020**, *21*, 429; doi:10.3390/ijms21020429

Tables and figures

Figure 1 Irradiation setup

Figure 2 Gold nanoparticle characterization

Figure 3 Gold nanoparticle association and toxicity with U87 GBM cells

Figure 4 Radiosensitization of U87 GBM by gold nanoparticles

Preprints (www.preprints.org) | NOT PEER-REVIEWED | Posted: 28 October 2019 doi:10.20944/preprints201910.0318.v1

Peer-reviewed version available at *Int. J. Mol. Sci.* **2020**, *21*, 429; doi:10.3390/ijms21020429

FIGURE 1: Irradiation setup

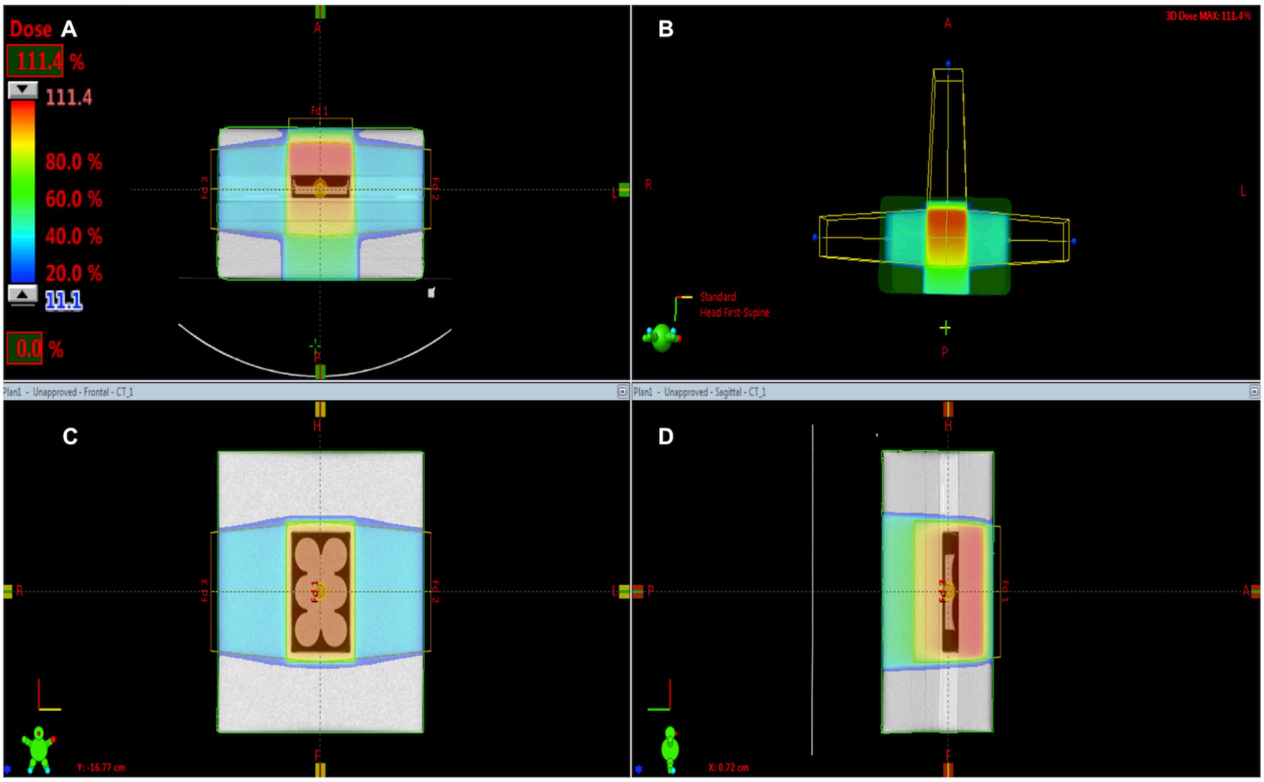

Figure 1: Irradiation setup

Demonstrates the dosimetry on Eclipse™ Treatment Planning System using a computed tomography (CT) simulation. (A) shows sagittal view of the CT simulation of well plates. The well plates are within the 95% isodose line (orange) indicating that at least 95% of prescribed dose is homogenously delivered to the GBM cells. (B) shows the 3-field technique (2 lateral opposed fields and single anterior field). (C) is an axial view to demonstrate the field size encompasses all 4 well plates. (D) shows the lateral view of bolus and plastic phantom.

Preprints (www.preprints.org) | NOT PEER-REVIEWED | Posted: 28 October 2019 doi:10.20944/preprints201910.0318.v1

Peer-reviewed version available at Int. J. Mol. Sci. 2020, 21, 429; doi:10.3390/ijms21020429

FIGURE 2: Gold nanoparticle characterization

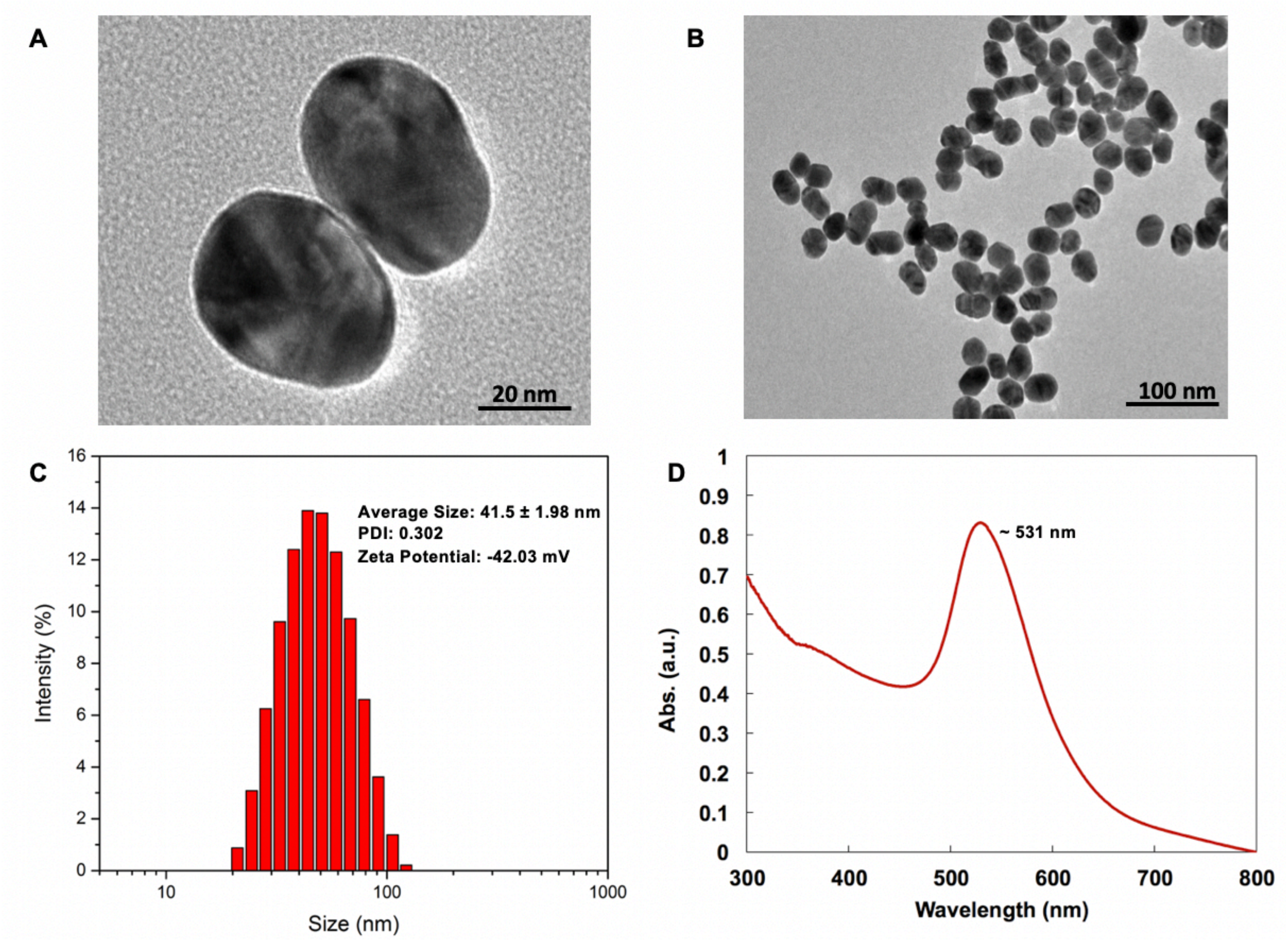

Figure 2: Gold nanoparticle characterization

Figures 2A and 2B show images from transmission electron microscopy of GNPs, at 25,000x and 40,000x magnification respectively, having diameter of approximately 42 nm. Figure 2C represents dynamic light scattering measurement of GNPs and shows sample was monodispersed. Figure 2D shows the UV-vis absorption spectrum of GNPs showing characteristic surface plasmon resonance at 531 nm.

Preprints (www.preprints.org) | NOT PEER-REVIEWED | Posted: 28 October 2019 doi:10.20944/preprints201910.0318.v1

Peer-reviewed version available at *Int. J. Mol. Sci.* **2020**, *21*, 429; doi:10.3390/ijms21020429

FIGURE 3: Gold nanoparticle association and cytoxicity with U87 GBM cells

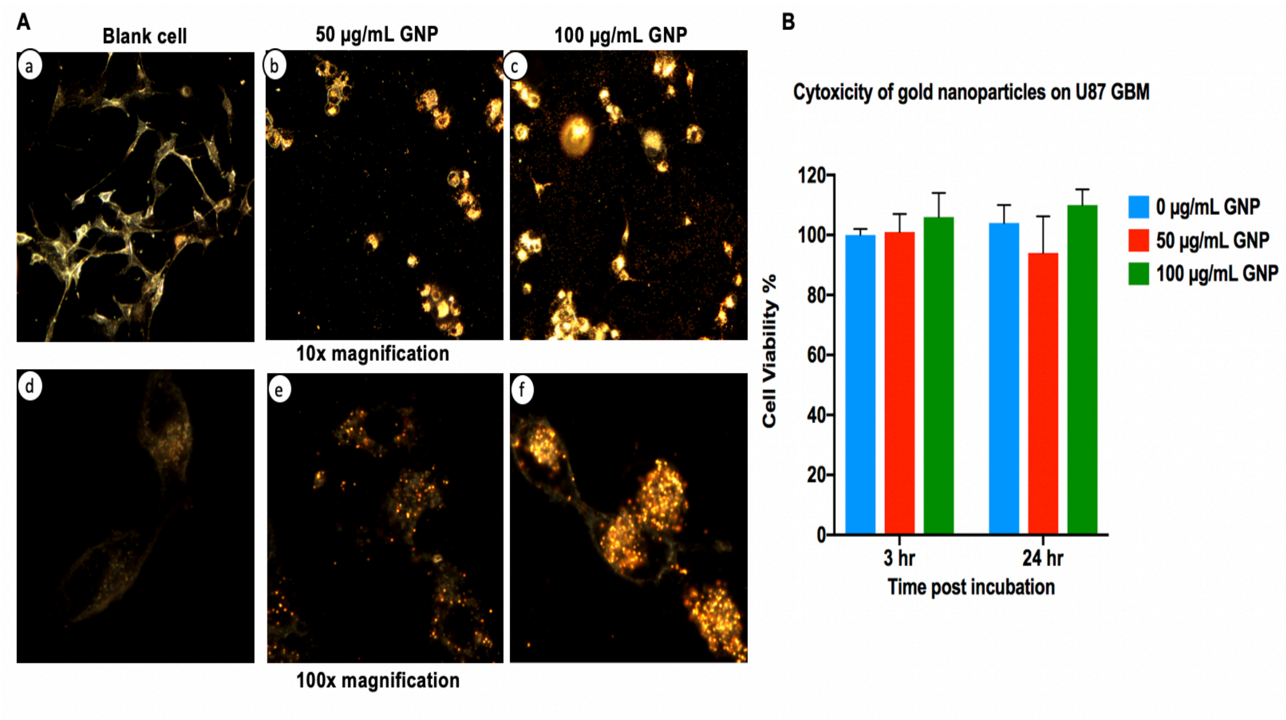

Figure 3: Gold nanoparticle association and cytoxicity with U87 GBM cells
Figure 3A shows images from dark field microscopy, under 10x magnification (panels a – c), a large number of gold nanoparticles were observed in association with the cells at the 100 µg/mL exposure level. Substantial amounts were also seen in 50 µg/mL samples. Under 100x magnification (panel d – f), increased GNP association with cells is observed with increasing concentrations of GNPs. Figure 3B shows MTS viability assay of U87 GBM cells pretreated with increasing concentrations of GNPs at 3 and 24 hours respectively. No significant difference (as tested by ANOVA, see methods) was observed between the 3 groups. Error bars represent standard deviation of mean for three independent repeats (n = 3).

Peer-reviewed version available at Int. J. Mol. Sci. 2020, 21, 429; doi:10.3390/ijms21020429

FIGURE 4: Radiosensitization of U87 GBM by gold nanoparticles

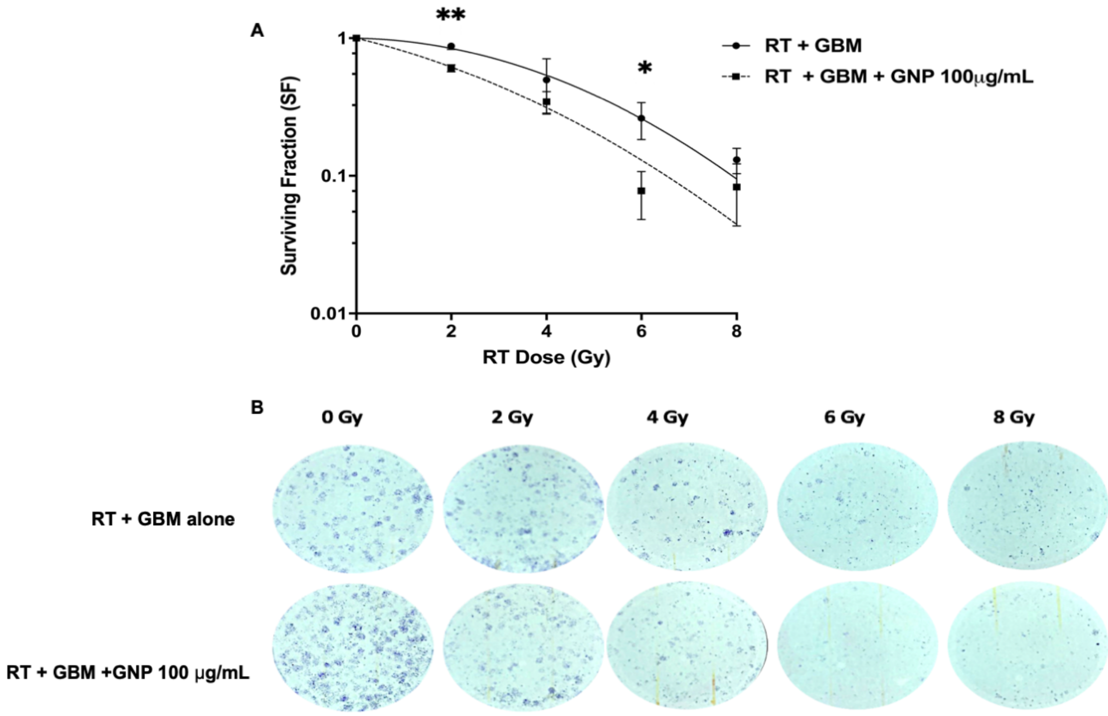

Figure 4: Radiosensitization of U87 GBM by gold nanoparticles:
Figure 4A represents the survival curves for U87 GBM cells irradiated with 6 MV X-rays. Data was fitted based on linear quadratic model comparing non-GNP treated group and GNP (100 µg/mL) treated group. Post irradiation 2000 cells were counted and plated. Error bars represent the standard deviation of mean for 3 independent experiments. Significance tested by multiple t test, * = p <0.05 and ** = p <0.01. Figure 4B shows representative images of the colonies for the GBM alone and GBM + GNP 100µg/mL at radiation dose 2, 4, 6 and 8 Gy. In the GBM alone group, the number of colonies formed at day 10 were 74, 66, 54, 19 and 10 at 0, 2, 4, 6, and 8 Gy respectively. In GBM + GNP 100 µg/mL wells, the number of colonies formed were 92, 62, 42, 8 and 8 at the respective radiation dose points.